

HE0359-3959: an extremely radiating quasar

M. L. Martínez-Aldama^{1,*}, A. Del Olmo¹, P. Marziani², C. A. Negrete³,
D. Dultzin⁴, M. A. Martínez-Carballo¹

¹Instituto de Astrofísica de Andalucía, IAA-CSIC, Granada, Spain

²INAF, Osservatorio Astronomico di Padova, Italy

³ CONACYT Research Fellow, Instituto de Astronomía, UNAM, Mexico

⁴Instituto de Astronomía, UNAM, Mexico

*Correspondence: maryloli@iaa.es

Abstract

We present a multiwavelength spectral study of the quasar HE0359-3959, which has been identified as an extreme radiating source at intermediate redshift ($z=1.5209$). Along the spectral range, the different ionic species give information about the substructures in the broad line region. The presence of a powerful outflow with an extreme blueshifted velocity of $\sim -6000 \pm 500$ km s⁻¹ is shown in the CIV λ 1549 emission line. A prominent blueshifted component is also associated with the 1900 Å blend, resembling the one observed in CIV λ 1549. We detect a strong contribution of very the low-ionization lines, FeII and Near-Infrared Ca II triplet. We find that the physical conditions for the low, intermediate and high-ionization emission lines are different, which indicate that the emission lines are emitted in different zones of the broad line region. The asymmetries shown by the profiles reveal different forces over emitter zones. The high-ionization region is strongly dominated by radiation forces, which also affect the low and intermediate-ionization emitter region, commonly governed by virial motions. These results support the idea that highly radiating sources host a slim disk.

Keywords: quasars: emission lines, quasars: outflows, quasars: individuals HE0359-3959.
quasars: supermassive black holes, galaxy evolution: feedback

1 Extreme Population A sources along the 4DE1 Main Sequence

The 4D Eigenvector 1 (4DE1) parameter space offers a formalism to distinguish and classify type 1 Active Galactic Nuclei (AGN) considering their spectral properties (Sulentic et al., 2000a,b). The Full Width at Half Maximum (FWHM) of $H\beta$ broad component ($H\beta_{BC}$), the strength of optical FeII blend at 4570\AA described by the ratio $R_{FeII} = I(FeII)/I(H\beta_{BC})$, the velocity shift of the $CIV\lambda 1549$ profile, and soft X-ray photon index (Γ_{soft}), provide four observationally independent dimensions of the Eigenvector 1. In the 4DE1 optical plane, the type 1 AGN occupy a well defined sequence, driven mainly by the Eddington ratio, L/L_{Edd} . Along this sequence we observe a variation of the physical parameters and orientation. Then, 4DE1 could be revealing an evolution sequence for type 1 AGN (Sulentic et al., 2000a; Marziani et al., 2010; Zamfir et al., 2010). For more information about the 4DE1 and update of results, see Marziani et al. 2017 in this volume.

Using the 4DE1 we identify two populations with different spectral features: A and B. Population A has a $FWHM(H\beta_{BC}) \leq 4000 \text{ km s}^{-1}$. It shows large blue asymmetries in the high-ionization lines like $CIV\lambda 1549$, and it is majority populated by radio quiet sources. In contrast, population B shows a $FWHM(H\beta_{BC}) > 4000 \text{ km s}^{-1}$ and it is mostly composed of radio-loud sources (Sulentic et al., 2002; Zamfir et al., 2010). Each population can be divided into small bins with $\Delta FWHM(H\beta_{BC}) = 4000 \text{ km s}^{-1}$ and $\Delta R_{FeII} = 0.5$, defining subpopulations shown in the Figure 1. In this paper we focus in the subpopulation A3 and A4 ($R_{FeII} > 1$), which have been identified as highly radiating sources (xA, Marziani & Sulentic, 2014). These kind of sources show high Eddington ratios ($L/L_{Edd} > 0.2$) probably produced by a slim disk, which is geometrically and optically thick and it could be formed in an advection-dominated accretion flow (Abramowicz et al., 1988; Abramowicz & Straub, 2014).

We have found selection criteria to identify the xA sources based on the 4DE1 formalism. In the optical region they show a $R_{FeII} > 1$ (high intensity of FeII) and in the UV range $AlIII\lambda 1860/SiIII\lambda 1892 \geq 0.5$ and $CIII\lambda 1909/SiIII\lambda 1892 \leq 1.0$ (Marziani & Sulentic, 2014). Also, they show strong blueshifted components associated with the high ionization lines, for example in $CIV\lambda 1549$ emission line, indicating the presence of outflows. More details about the xA sources behavior can be found in Martínez-Aldama et al. of this volume.

1.1 HE0359-3959: an extreme xA source

In our extreme luminosity Hamburg-ESO sample (Marziani et al., 2009; Sulentic et al., 2017), we have identified four cases of highly radiating quasars that show an extreme behavior, i.e., a high Eddington ratio and a strong blue asymmetry ($c^{(1/2)} < -4000 \text{ km s}^{-1}$; centroid at half intensity) in the $CIV\lambda 1549$ profile (Sulentic et al., 2017). The most extreme case corresponds to the quasars HE0359-3959, with $z=1.5209$, $\log(L_{bol})=47.6 \text{ erg s}^{-1}$ and a $R_{FeII}=1.12$. It is cataloged as an A3 source (see Figure 1).

The aim of this paper is to analyze the spectral behavior of an extreme xA source, the quasar HE0359–3959. We performed multicomponent fits in a wide spectral range: UV, optical and Near–Infrared (Section 2); which gives us information about the dynamics and the physical conditions of the broad line region (BLR) (Section 3). In Section 4, we summarize the main results of our work.

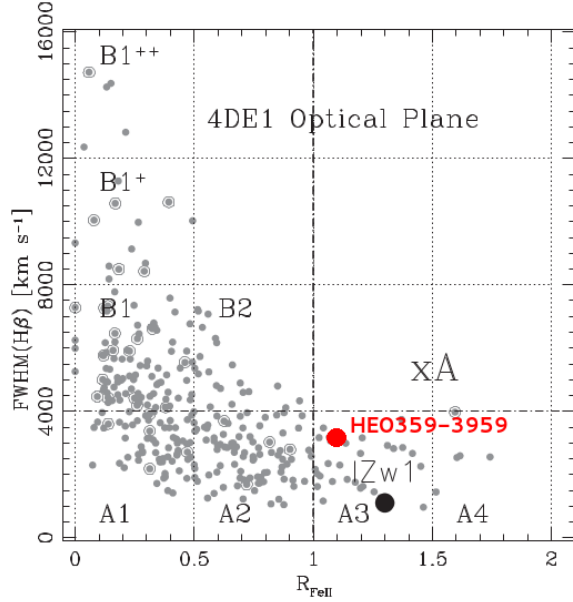


Figure 1: 4DE1 Optical Plane reproduced from Marziani & Sulentic (2014). Grey points correspond to the sample of 470 bright low- z QSOs from Zamfir et al. (2010). The plane is divided in bins according to Sulentic et al. (2002). Extreme accretor population A sources (xA) are located in A3 and A4 bins. The black dot indicates the position of 1 Zw 1, the prototype of low- z xA sources. And, the red dot marks the location of HE0359-3959, an extreme xA source with high- z .

2 Observations, data reduction and multicomponent fitting

2.1 Observations and data reduction

Ultraviolet (UV), optical and Near–Infrared spectra were observed with the Very Large Telescope (VLT-ESO). Optical and Near–Infrared spectra were obtained with the Infrared Spectrometer And Array Camera (ISAAC; decommissioned in 2013) using a slit of $0.6''$. The near–infrared spectrum was observed in 2010 in the K band with a total exposure time of 1120 seconds. The

optical spectrum was observed in 2004 in the J band with a total exposure time of 3600 seconds. For the ultraviolet spectrum we used the Focal Reducer and low dispersion Spectrograph (FORS1) a slit of $1.0''$ with a total exposure time of 1440 seconds. It was observed in 2008. The data reduction was done using the IRAF package. The procedures followed are explained in Marziani et al. (2009), Martínez-Aldama et al. (2015) and Sulentic et al. (2017).

2.2 Multicomponent fits

We perform multicomponent fits using SPECFIT, an IRAF routine (Kriss, 1994) to get the information of the most important emission lines. In each spectral range we fit a local continuum. The FWHM of all the broad components (BC) for $H\beta$, $\text{AlIII}\lambda 1860$, $\text{SiIII}\lambda 1892$, $\text{CIV}\lambda 1549$ and $\text{SiIV}\lambda 1397$ was taken equal. In the Figure 2, we present the multicomponents fits after continuum subtraction, for the $\text{CIV}\lambda 1549$ and Ca II triplet range. The rest of the fits will be shown in an upcoming paper.

3 Results

3.1 Multiwavelength analysis

Low-ionization lines (LIL) have an ionization potential (IP) ≤ 20 eV. The $H\beta$ line is the prototype of LIL. In population A3 and A4 sources $H\beta$ has associated a blueshifted component (Bachev et al., 2004). In the case of HE0359-3959, the blueshifted component has a contribution to the total flux of $\sim 9\%$, and shows a centroid a half intensity of $c(1/2) \approx -500 \pm 70 \text{ km s}^{-1}$.

The FeII (IP ~ 16 eV) has an important contribution in the optical and near-infrared regions. To reproduce it we used the templates modeled by Marziani et al. (2009) and García-Rissmann et al. (2012) for the optical and near-infrared ranges, respectively. Several works have found (Joly, 1989; Persson, 1988; Ferland & Persson, 1989; Dultzin et al., 1999; Martínez-Aldama et al., 2015) a close relationship between the FeII and the NIR Ca II $\lambda 8498, \lambda 8542$ and $\lambda 8662 \text{ \AA}$ triplet. This relation is very well appreciable in this object: as well as the optical FeII is strong, the NIR Ca II triplet also is. It is the first time where we observe the Ca II triplet lines isolated at high redshift. Strong intensities of both ions imply an extremely low-ionization degree ($U < 10^{-2}$; U : ionization parameter) and a high density ($n_{\text{H}} \sim 10^{11-13} \text{ cm}^{-3}$) (Baldwin et al., 2004; Matsuoka et al., 2007; Martínez-Aldama et al., 2015).

In the UV region, the 1900\AA blend is formed by two intermediate-ionization lines (IIL; IP $\sim 20-40$ eV), $\text{AlIII}\lambda 1860$ and $\text{SiIII}\lambda 1892$, which are accompanied by $\text{CIII}\lambda 1909$ and some FeIII transitions. In this blend we appreciate a blueshifted component. This component should be most likely associated with $\text{AlIII}\lambda 1860$. Respect to $\text{AlIII}\lambda 1860$, the blueshifted component has a contribution of the total profile of 60% . The centroid a half intensity is $c(1/2) \approx -3200 \pm 250 \text{ km s}^{-1}$, which indicates the presence of an outflow generated by radiation forces presented in the intermediate-ionization lines (Marziani et al., 2017). On the other hand, considering the high intensity of $\text{AlIII}\lambda 1860$, $\text{SiIII}\lambda 1892$, Ca II and FeII , it could suggest a possible chemical

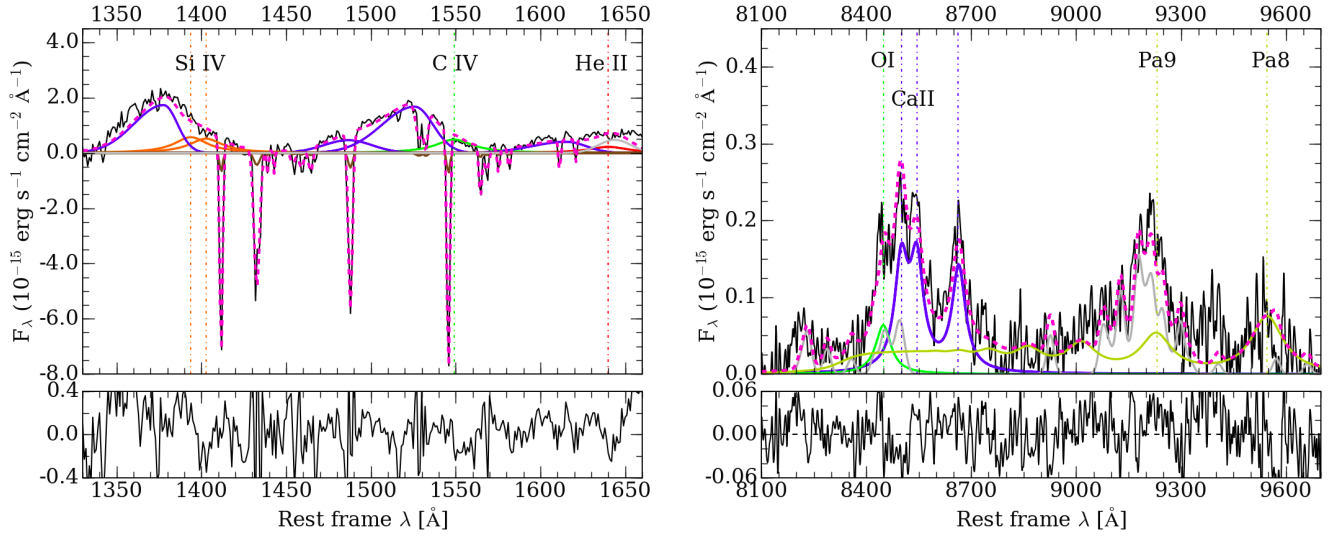


Figure 2: Multicomponent analysis on the UV, optical and NIR spectra of HE0359-3959 after continuum subtraction. TOP PANELS: In the left side is shown the UV spectrum, while in the right one is shown the near-infrared spectrum. The different components (broad (BC), BLUE, and narrow (NC)) in the line fitting are specified in each panel. Vertical lines indicate the rest-frame obtained through $H\beta_{NC}$. The gray line marks the FeII contribution. The vertical scale represents the relative flux in units of $10^{-15} \text{ erg s}^{-1} \text{ cm}^{-2} \text{ \AA}^{-1}$. BOTTOM PANEL: Residuals of the fittings. The horizontal scale is the radial velocity shift in km s^{-1} . In all the panels the horizontal scale represents the rest-frame wavelength in \AA .

enrichment of the BLR (Juarez et al., 2009).

High ionization lines (HIL; $IP > 40$ eV), C IV $\lambda 1549$, He II $\lambda 1640$ and Si IV $\lambda 1397$, show a prominent blueshifted component. We find that the blue component has a contribution of 76%, 62% and 57% to the total flux of C IV $\lambda 1549$, He II $\lambda 1640$ and Si IV $\lambda 1397$ respectively. The C IV $\lambda 1549$ reaches $c(1/2) \sim -6000 \pm 500$ km s $^{-1}$, while He II $\lambda 1640$ and Si IV $\lambda 1397$ $c(1/2) \sim -4000 \pm 550$ km s $^{-1}$. The velocities reached are ones of the highest found in the literature (Richards et al., 2011; Coatman et al., 20016; Sulentic et al., 2017). Then, it indicates that the full profile is dominated by an outflow and suggests the disk plus wind scenario (Gaskell, 1982; Richards et al., 2002, 2011).

3.2 Physical properties of HE0359-3959

In order to study the physical properties of the quasar HE0359-3959, we built a grid of photoionization simulations using the CLOUDY code (Ferland et al., 1998, 2013). For our simulations we consider a Mathews and Ferland continuum (Mathews & Ferland, 1987), a plane-parallel geometry, a metallicity $5Z_{\odot}$ with an overabundance of Al and Si with respect to carbon (by a factor of three), and a column density of $N_c = 10^{23}$ cm $^{-2}$. See Negrete et al. (2012) for more details. Our simulations span the density range $7.00 \leq \log(n_H) \leq 14.00$ and $-4.5 \leq \log(U) \leq 0.00$ for the ionization parameter, in intervals of 0.25 dex. More details about the CLOUDY simulations can be found in Negrete et al. (2014). Using the UV lines, we define three groups of diagnostic ratios:

- The flux ratio Al III $\lambda 1860$ /Si III $\lambda 1892$ is a useful density diagnostic.
- The flux ratio Si IV $\lambda 1397$ /Si III $\lambda 1892$ for the ionization parameter.
- The flux ratio C IV $\lambda 1549$ /Si IV $\lambda 1397$ is mainly sensitive to the relative abundances of C and Si.

In Figure 3 is shown the result of the simulations. We obtained that the flux ratios are intersected in $\log(n_H) = 12.32$ cm $^{-3}$ and $\log(U) = -2.95$. Compared to not highly radiating AGNs (Negrete et al., 2013), this source shows a high density and a low ionization parameter, which marks a different behavior in the BLR, probably causing by the slim disk hosted in these kind of sources. Taking into account the high intensity of Al III $\lambda 1860$, Fe II and Ca II we conclude that effectively the low-ionization emitter zone has a high density and low-ionization parameter.

Negrete et al. (2012) proposed a new method to determine the size of the BLR (r_{BLR}) and the black hole mass (M_{BH}) based on the product $n_H \cdot U$ and independently of redshift. This method gives similar results to the obtained from the classical methods such as reverberation mapping at low- z (Negrete et al., 2014). Knowing the product of $n_H \cdot U$ obtained from the CLOUDY simulations, we compute the size of the BLR (r_{BLR}) and considering the FWHM of the broad components as the velocity dispersion, we can get the black hole mass (M_{BH}) and the Eddington ratio. The size of the BLR is $\log(r_{\text{BLR}}) = 18.37 \pm 0.04$ cm and the black hole mass is

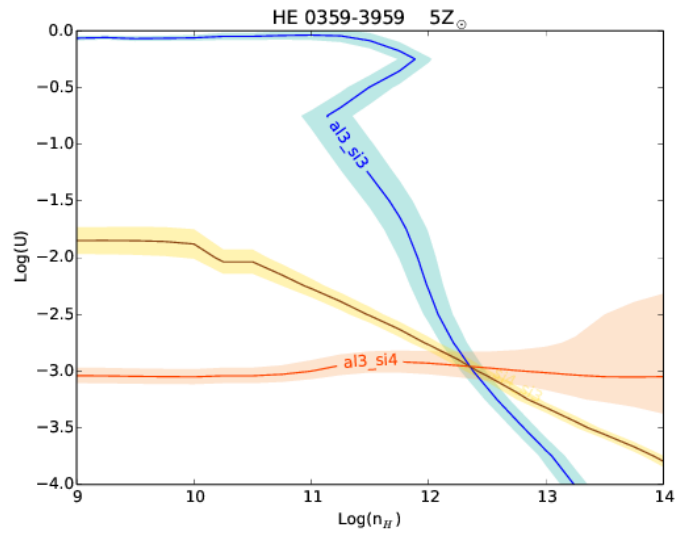


Figure 3: Isocontours for HE0359-3959 with $5Z_{\odot}$ and an overabundance of Al and Si. The blue line indicates the flux ratio $\text{AlIII}\lambda 1860/\text{SiIII}\lambda 1892$, the yellow one indicates the ratio $\text{SiIV}\lambda 1397/\text{SiIII}\lambda 1892$ and the orange corresponds to the $\text{AlIII}\lambda 1860/\text{SiIV}\lambda 1397$. Shadows associated with each line indicate the error. The flux ratios are intersected in $n_{\text{H}} \cdot U = 9.27 \pm 0.39$

$\log(M_{\text{BH}})=9.52\pm 0.41 M_{\odot}$. These values are in agreement with the ones found for a large xA sample at high-redshift (Martínez-Aldama et al. in prep.).

The Eddington ratio for this source is $L/L_{\text{Edd}}=0.74\pm 0.11$. Considering that it shows a $c^{(1/2)}\sim -6000\pm 500 \text{ km s}^{-1}$ for $\text{CIV}\lambda 1549$, we confirm the directly proportional relation between $c^{(1/2)}$ and L/L_{Edd} . Indicating that L/L_{Edd} could be the driver of the outflows (Sulentic et al., 2017).

4 Conclusions

The information given by the multiwavelength analysis indicates that in HE0359–3959 there is coexistence of substructures in the broad line region. Low and intermediate-ionization regions, where $\text{H}\beta$, $\text{AlIII}\lambda 1860$ and $\text{SiIII}\lambda 1892$ are emitted, are dense ($n_{\text{H}}\sim 10^{11-12} \text{ cm}^{-3}$) and optically thick ($U\sim 10^{-2.5}$). They are mainly governed by virial motions and the presence of a blueshifted component indicates the influence of radiation forces. On the other hand, according to Marziani et al. (2010) the high-ionization region is less dense ($n_{\text{H}}\sim 10^{10} \text{ cm}^{-3}$, $U\sim 10^{-1}$), pointing out a difference with the physical conditions shown by the low and intermediate-ionization lines.

High ionization lines are dominated by strong radiation forces, producing outflows in high-ionization lines like $\text{CIV}\lambda 1549$, $\text{HeII}\lambda 1640$ and $\text{SiIV}\lambda 1397$. The high Eddington ratio value suggests the presence of a slim optically thick disk which could be related to the extreme outflow properties observed in HE0359-3959. The presence of strong outflows has been related with the co-evolution of the active galactic nuclei and the host galaxy.

Acknowledgements. M.L.M.A acknowledge the postdoctoral grant from CONACyT. M.L.M.A., A.d.O. and M.A.M.C. acknowledge financial support from Spanish Ministry for Economy and Competitiveness through grants AYA2013-42227-P and AYA2016-76682-C3-3-1-P.

References

- ABRAMOWICZ, M. A., Czerny, B., Lasota, J. P. and Szuszkiewicz, E., 1988, *Astrophys. J.*, 332, 646-658
- ABRAMOWICZ, M. A. & Straub, O., 2014, 9
- BACHEV, R., Marziani, P., Sulentic, J. W., Zamanov, R., Calvani, M. and Dultzin-Hacyan, D., 2004, *Astrophys. J.*, 617, 171-183
- BALDWIN, J. A., Ferland, G. J., Korista, K. T., Hamann, F. and LaCluyz e, A., 2004, *Astrophys. J.*, 615, 610-624
- COATMAN, L. and Hewett, P. C. and Banerji, M. and Richards, G. T., 2016, *Mon. Not. Roy. Astron. Soc.*, 461, 647-665

- DULTZIN-HACYAN, D., Taniguchi, Y. and Uranga, L., 1999, *PASP*, 175, 303
- FERLAND, G. J. & Persson, S. E., 1989, *Astrophys. J.*, 347, 656-673
- FERLAND, G. J., Korista, K. T., Verner, D. A., Ferguson, J. W., Kingdon, J. B. and Verner, E. M., 1998, *PASP*, 110, 761-778
- FERLAND, G. J., Hu, C., Wang, J.-M., Baldwin, J. A., Porter, R. L., van Hoof, P. A. M. and Williams, R. J. R., 2009, *Astrophys. J.*, 707, L82-L86
- FERLAND, G. J., Porter, R. L., van Hoof, P. A. M., Williams, R. J. R., Abel, N. P., Lykins, M. L., Shaw, G., Henney, W. J. and Stancil, P. C., 2013, *RMxAA*, 49, 137-163
- GARCÍA-RISSMANN, A., Rodríguez-Ardila, A. and Sigut, T. A. A. and Pradhan, A. K., 2012, *Astrophys. J.*, 751, 7
- GASKELL, C. M., 1982, *Astrophys. J.*, 263, 79-86
- JOLY, M., 1989, *Astron. Astrophys.*, 208, 47-51
- JUAREZ, Y., Maiolino, R., Mujica, R., Pedani, M., Marinoni, S., Nagao, T., Marconi, A. and Oliva, E., 2009, *Astron. Astrophys.*, 494, L4-L28
- KRISS, G., 1994, *Astronomical Data Analysis Software and Systems*, 3, 437
- MARTÍNEZ-ALDAMA, M. L., Dultzin, D., Marziani, P., Sulentic, J. W., Bressan, A., Chen, Y. and Stirpe, G. M., 2015, *Astrophys. J. S.*, 217, 3
- MARZIANI, P., Sulentic, J. W., Zwitter, T., Dultzin-Hacyan, D. and Calvani, M., 2001, *Astrophys. J.*, 558, 553-560
- MARZIANI, P., Sulentic, J. W., Stirpe, G. M., Zamfir, S. and Calvani, M., 2009, *Astron. Astrophys.*, 495, 83-112
- MARZIANI, P., Sulentic, J. W., Negrete, C. A., Dultzin, D., Zamfir, S. and Bachev, R., 2010, 409, 1033-1048
- MARZIANI, P. & Sulentic, J. W., 2014, *Mon. Not. Roy. Astron. Soc.*, 442, 1211-1229
- MARZIANI, P., Del Olmo, A., Martnez-Aldama, M. L., Dultzin, D., Negrete, C., Bon, E., Bon, N. and D'Onofrio, M., 2017, *Atoms*, 5, 33-47
- MATSUOKA, Y., Oyabu, S., Tsuzuki, Y. and Kawara, K., 2007, *Astrophys. J.*, 663, 781-798
- MATSUOKA, Y., Kawara, K. and Oyabu, S., 2008, *Astrophys. J.*, 673, 62-68
- MATHEWS, W. G. & Ferland, G. J., 1987, *Astrophys. J.*, 323, 456-467
- NEGRETE, C. A., Dultzin, D., Marziani, P. and Sulentic, J. W., 2012, *Astrophys. J.*, 757, 62

- NEGRETE, C. A., Dultzin, D., Marziani, P. and Sulentic, J. W., 2013, *Astrophys. J.* 771, 31
- NEGRETE, C. A., Dultzin, D., Marziani, P. and Sulentic, J. W., 2014, *Astrophys. J.*, 794, 95
- PERSSON, S. E., 1988, *Astrophys. J.*, 330, 751-765
- RICHARDS, G. T., Vanden Berk, D. E., Reichard, T. A., Hall, P. B., Schneider, D. P., SubbaRao, M., Thakar, A. R. and York, D. G., 2002, *Astrophys. J.*, 124, 1-17
- RICHARDS, G. T., Kruczek, N. E., Gallagher, S. C., Hall, P. B., Hewett, P. C., Leighly, K. M., Deo, R. P., Kratzer, R. M. and Shen, Y., 2011, *Astrophys. J.*, 141, 167
- SHEN, Y. & Ho, L. C., 2014, *Nature*, 513, 210-213
- SHIN, J., Kim, S. S. and Yoon, S.-J. and Kim, J., 2013, *Astrophys. J.*, 762, 135
- SULENTIC, J. W., Marziani, P. and Dultzin-Hacyan, D., 2000a, *Annu. Rev. Astron. Astrophys.*, 38, 521-571
- SULENTIC, J. W., Zwitter, T., Marziani, P. and Dultzin-Hacyan, D., 2000b, *Astrophys. J.*, 536, L5-L9
- SULENTIC, J. W., Marziani, P., Zamanov, R., Bachev, R., Calvani, M. and Dultzin-Hacyan, D., 2002, *Astrophys. J.*, 566, L71-L75
- SULENTIC, J. W., Bachev, R., Marziani, P., Negrete, C. A. and Dultzin, D., 2007, *Astrophys. J.*, 666, 757-777
- SULENTIC, J., Marziani, P. and Zamfir, S., 2011, *Baltic Astronomy*, 20, 427-434
- SULENTIC, J. W., Del Olmo, A., Marziani, P., Martínez-Carballo, M. A., D'Onofrio, M., Dultzin, D., Martínez-Aldama, M. L., Negrete, C., Stirpe, G. M. and Zamfir, S., 2017, *Astron. & Astrophys.*, 608, 122
- VIETRI, G., 2017, *American Astronomical Society Meeting*, 229, 302
- ZAMFIR, S., Sulentic, J. W., Marziani, P. and Dultzin, D., 2010, *Mon. Not. Roy. Astron. Soc.*, 403, 1759-1786